 CMES, vol.54, no.3, pp.335-368, 2009

Large Deformation Analyses of Space-Frame Structures, Using Explicit Tangent Stiffness Matrices, Based on the Reissner variational principle and a von Karman Type Nonlinear Theory in Rotated Reference Frames

Yongchang Cai[1,2], J.K. Paik[3] and Satya N. Atluri[3]

Abstract: This paper presents a simple finite element method, based on assumed moments and rotations, for geometrically nonlinear large rotation analyses of space frames consisting of members of arbitrary cross-section. A von Karman type nonlinear theory of deformation is employed in the updated Lagrangian co-rotational reference frame of each beam element, to account for bending, stretching, and torsion of each element. The Reissner variational principle is used in the updated Lagrangian co-rotational reference frame, to derive an explicit expression for the (12x12) *symmetric* tangent stiffness matrix of the beam element in the co-rotational reference frame. The explicit expression for the finite rotation of the axes of the co-rotational reference frame, from the global Cartesian reference frame is derived from the finite displacement vectors of the 2 nodes of each finite element. Thus, the explicit expressions for the tangent stiffness matrix of each finite element of the beam, in the global Cartesian frame, can be seen to be derived as text-book examples of nonlinear analyses. When compared to the primal (displacement) approach wherein C^1 continuous trial functions (for transverse displacements) over each element are neccessary, in the current approch the trial functions for the transverse bending moments and rotations are very simple, and can be assumed to be linear within each element. The present (12×12) symmetric tangent stiffness matrices of the beam, based on the Reissner variational principle and the von Karman type simplified rod theory, are much simpler than those of many others in the literature. The present approach does not involve such numerical procedures as selective reduced integration or suppression of attendant Kinematic modes. The present methodolo-

[1] Key Laboratory of Geotechnical and Underground Engineering of Ministry of Education, Department of Geotechnical Engineering, Tongji University, Shanghai 200092, P.R.China. E-mail: yc_cai@163.net

[2] Center for Aerospace Research & Education, University of California, Irvine

[3] Lloyd's Register Educational Trust (LRET) Center of Excellence, Pusan National University, Korea

gies can be extended to study the very large deformations of plates and shells as well. Metal plasticity may also be included, through the method of plastic hinges, etc. This paper is a tribute to the collective genius of Theodore von Karman (1881-1963) and Eric Reissner (1913-1996).

Keywords: Large deformation, Unsymmetrical cross-section, Explicit tangent stiffness, Updated Lagrangian formulation, Rod, Space frames, Reissner variational principle

1 Introduction

In the past decades, large deformation analyses of space frames have attracted much attention due to their significance in diverse engineering applications. Many different methods were developed by numerous researchers for the geometrically nonlinear analyses of 3D frame structures. Bathe and Bolourchi (1979) employed the total Lagrangian and updated Lagrangian approaches to formulate fully nonlinear 3D continuum beam elements. Punch and Atluri (1984) examined the performance of linear and quadratic Serendipity hybrid-stress 2D and 3D beam elements. Based on geometric considerations, Lo (1992) developed a general 3D nonlinear beam element, which can remove the restriction of small nodal rotations between two successive load increments. Kondoh, Tanaka and Atluri (1986), Kondoh and Atluri (1987), Shi and Atluri(1988) presented the derivations of explicit expressions of the tangent stiffness matrix, without employing either numerical or symbolic integration. Zhou and Chan (2004a, 2004b) developed a precise element capable of modeling elastoplastic buckling of a column by using a single element per member for large deflection analysis. Izzuddin (2001) clarified some of the conceptual issues which are related to the geometrically nonlinear analysis of 3D framed structures. Simo (1985), Mata, Oller and Barbat (2007, 2008), Auricchio, Carotenuto and Reali (2008) considered the nonlinear constitutive behavior in the geometrically nonlinear formulation for beams. Iura and Atluri (1988), Chan (1994), Xue and Meek (2001), Wu, Tsai and Lee(2009) studied the nonlinear dynamic response of the 3D frames. Lee, Lin, Lee, Lu and Liu (2008), Lee, Lu, Liu and Huang (2008), Lee and Wu (2009) gave the exact large deflection solutions of the beams for some special cases. Gendy and Saleeb (1992); Atluri, Iura, and Vasudevan(2001) had brief discussions of arbitrary cross sections. Dinis, Jorge and Belinha (2009), Han, Rajendran and Atluri (2005), Lee and Chen (2009), Rabczuk and Areias (2006), Shaw and Roy (2007), Wen and Hon (2007) applied meshless methods to the analyses of nonlinear problems with large deformations or rotations. Large rotations in beams, plates and shells, and attendant variational principles involving the rotation tensor as a direct variable, were studied extensively by Atluri and his co-workers

(see, for instance, Atluri 1980, Atluri 1984, and Atluri and Cazzani 1994).

This paper presents a simple finite element method, based on assumed moments and rotations, for geometrically nonlinear large rotation analyses of space frames consisting of members of arbitrary cross-section. A von Karman type nonlinear theory of deformation is employed in the updated Lagrangian co-rotational reference frame of each beam element, to account for bending, stretching, and torsion of each element. The Reissner variational principle (1953) [see also Atluri and Reissner (1989)] is used in the updated Lagrangian co-rotational reference frame, to derive an explicit expression for the (12x12) *symmetric* tangent stiffness matrix of the beam element in the co-rotational reference frame. The explicit expression for the finite rotation of the axes of the co-rotational reference frame, from the global Cartesian reference frame is derived from the finite displacement vectors of the 2 nodes of each finite element. Thus, the explicit expressions for the tangent stiffness matrix of each finite element of the beam, in the global Cartesian frame, can be seen to be derived as text-book examples of nonlinear analyses. When compared to the primal (displacement) approach wherein C^1 continuous trial functions (for transverse displacements) over each element are necessary, in the current approach the trial functions for the transverse bending moments and rotations are very simple, and can be assumed to be linear within each element. The present (12×12) symmetric tangent stiffness matrices of the beam, based on the Reissner variational principle and the von Karman type simplified rod theory, are much simpler than those of many others in the literature, such as, Simo (1985), Bathe and Bolourchi (1979), Kondon, Tanaka and Atluri (1986), Kondoh and Atluri (1987), and Shi and Atluri (1988). The present approach does not involve such numerical procedures as selective reduced integration or suppression of attendant Kinematic modes. The present methodologies can be extended to study the very large deformations of plates and shells as well. Metal plasticity may also be included, through the method of plastic hinges, etc. Furthermore, Unlike in the formulations of Simo(1985), Crisfield (1990) [and many others who followed them], which lead to the currently popular myth that the stiffness matrices of finitely rotated structural members should be *unsymmetric*, the (12x12) stiffness matrix of the beam element in the present paper is enormously simple, and remains *symmetric* throughout the finite rotational deformation. This paper is a tribute to the collective genius of Theodore von Karman (1881-1963) and Eric Reissner (1913-1996).

2 Von-Karman type nonlinear theory for a rod with large deformations

We consider a fixed global reference frame with axes $\bar{x}_i\,(i=1,2,3)$ and base vectors $\bar{\mathbf{e}}_i$. An initially straight rod of an arbitrary cross-section and base vectors $\tilde{\mathbf{e}}_i$, in its undeformed state, with local coordinates $\tilde{x}_i\,(i=1,2,3)$, is located arbitrarily in

space, as shown in Fig.1. The current configuration of the rod, after arbitrarily large deformations (but small strains) is also shown in Fig.1.

The local coordinates in the reference frame in the current configuration are x_i and the base vectors are $\mathbf{e}_i\,(i=1,2,3)$. The nodes 1 and 2 of the rod (or an element of the rod) are supposed to undergo arbitrarily large displacements, and the rotations between the $\tilde{\mathbf{e}}_i\,(i=1,2,3)$ and the $\mathbf{e}_k\,(k=1,2,3)$ base vectors are assumed to be arbitrarily finite. In the continuing deformation from the current configuration, the local displacements in the $x_i\,(\mathbf{e}_i)$ coordinate system are assumed to be moderate, and the local gradient $(\partial u_{10}/\partial x_1)$ is assumed to be small compared to the transverse rotations $(\partial u_{\alpha 0}/\partial x_1)\,(\alpha=2,3)$. Thus, in essence, a von-Karman type deformation is assumed for the continued deformation from the current configuration, in the co-rotational frame of reference $\mathbf{e}_i\,(i=1,2,3)$ in the local coordinates $x_i\,(i=1,2,3)$. If H is the characteristic dimension of the cross-section of the rod, the precise assumptions governing the continued deformations from the current configuration are

$$\frac{u_{10}}{H}\ll 1;\quad \frac{H}{L}\ll 1$$

$$\frac{u_{\alpha 0}}{H}\approx \mathrm{O}\,(1)\,(\alpha=2,3)$$

$$\frac{\partial u_{10}}{\partial x_1}\ll \frac{\partial u_{\alpha 0}}{\partial x_1}\ (\alpha=2,3)$$

and $\left(\frac{\partial u_{\alpha 0}}{\partial x_1}\right)^2\ (\alpha=2,3)$ are not negligible.

As shown in Fig.2, we consider the large deformations of a cylindrical rod, subjected to bending (in two directions), and torsion around x_1. The cross-section is unsymmetrical around x_2 and x_3 axes, and is constant along x_1.

As shown in Fig.2, the warping displacement due to the torque T around x_1 axis is $u_{1T}\,(x_2,x_3)$ and does not depend on x_1, the axial displacement at the origin ($x_2=x_3=0$) is $u_{10}\,(x_1)$, and the bending displacement at $x_2=x_3=0$ along the axis x_1 are $u_{20}\,(x_1)$ (along x_2) and $u_{30}\,(x_1)$ (along x_3).

We consider only loading situations when the generally 3-dimensional displacement state in the $\mathbf{e}_i$ system, donated as

$$u_i=u_i\,(x_k)\quad i=1,2,3;\quad k=1,2,3$$

is simplified to be of the type:

$$\begin{aligned} u_1&=u_{1T}\,(x_2,x_3)+u_{10}\,(x_1)-x_2\frac{\partial u_{20}}{\partial x_1}-x_3\frac{\partial u_{30}}{\partial x_1}\\ u_2&=u_{20}\,(x_1)-\hat{\theta}x_3\\ u_3&=u_{30}\,(x_1)+\hat{\theta}x_2 \end{aligned} \tag{1}$$

where $\hat{\theta}$ is the total torsion of the rod at x_1 due to the torque T.

2.1 Strain-displacement relations

Considering only von Karman type nonlinearities in the rotated reference frame $\mathbf{e}_i\,(x_i)$, we can write the Green-Lagrange strain-displacement relations in the updated Lagrangian co-rotational frame $\mathbf{e}_i$ in Fig.1 as:

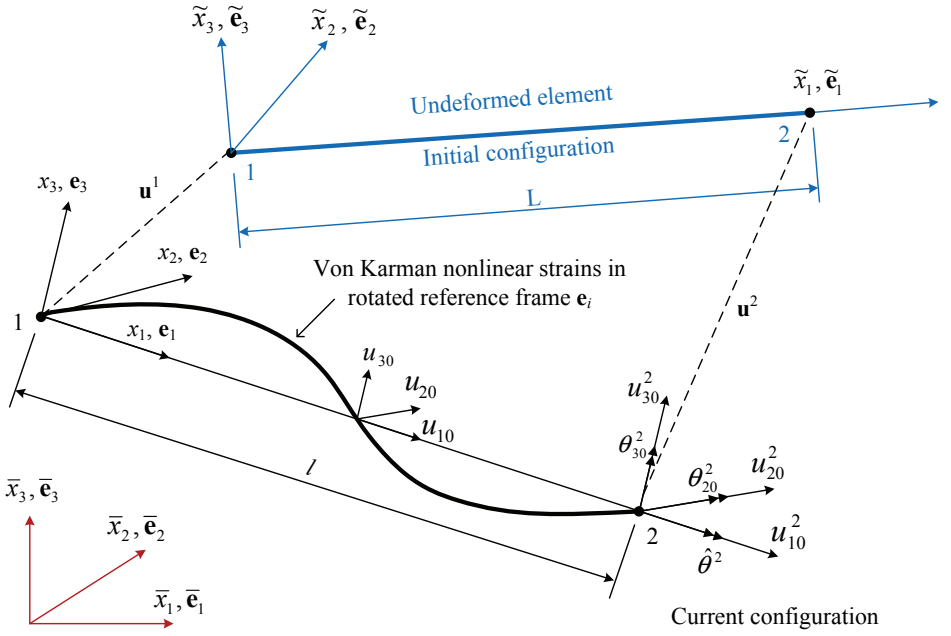

Figure 1: Kinematics of deformation of a space framed member

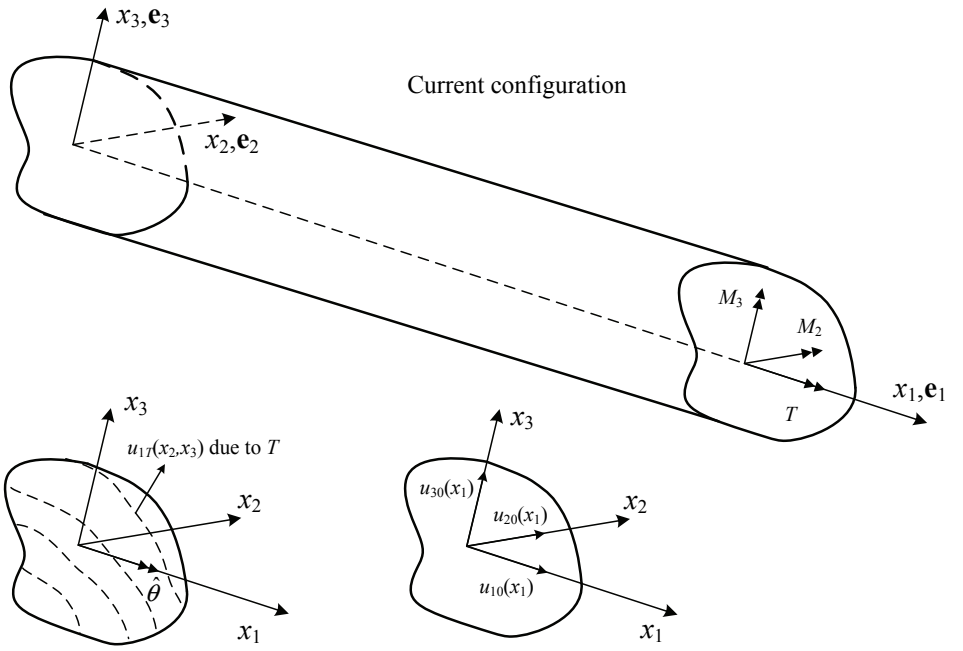

Figure 2: Large deformation analysis model of a cylindrical rod

$$
\begin{aligned}
\varepsilon_{11} &= \frac{\partial u_1}{\partial x_1} + \frac{1}{2}\left(\frac{\partial u_2}{\partial x_1}\right)^2 + \frac{1}{2}\left(\frac{\partial u_3}{\partial x_1}\right)^2 \\
&= \frac{\partial u_{10}}{\partial x_1} + \frac{1}{2}\left(\frac{\partial u_{20}}{\partial x_1}\right)^2 + \frac{1}{2}\left(\frac{\partial u_{30}}{\partial x_1}\right)^2 - x_2\frac{\partial^2 u_{20}}{\partial x_1^2} - x_3\frac{\partial^2 u_{30}}{\partial x_1^2} \\
\varepsilon_{12} &= \frac{1}{2}\left(\frac{\partial u_1}{\partial x_2} + \frac{\partial u_2}{\partial x_1}\right) \\
&= \frac{1}{2}\left(\frac{\partial u_{1T}}{\partial x_2} - \frac{\partial u_{20}}{\partial x_1} + \frac{\partial u_{20}}{\partial x_1} - \frac{\partial \hat{\theta}}{\partial x_1}x_3\right) = \frac{1}{2}\left(\frac{\partial u_{1T}}{\partial x_2} - \theta\ x_3\right) \\
\varepsilon_{13} &= \frac{1}{2}\left(\frac{\partial u_1}{\partial x_3} + \frac{\partial u_3}{\partial x_1}\right) \\
&= \frac{1}{2}\left(\frac{\partial u_{1T}}{\partial x_3} - \frac{\partial u_{30}}{\partial x_1} + \frac{\partial u_{30}}{\partial x_1} + \theta x_2\right) = \frac{1}{2}\left(\frac{\partial u_{1T}}{\partial x_3} + \theta x_2\right) \\
\varepsilon_{22} &= \frac{\partial u_2}{\partial x_2} + \frac{1}{2}\left(\frac{\partial u_1}{\partial x_2}\right)^2 + \frac{1}{2}\left(\frac{\partial u_2}{\partial x_2}\right)^2 + \frac{1}{2}\left(\frac{\partial u_3}{\partial x_2}\right)^2 \\
&\approx 0 + \frac{1}{2}\left(\frac{\partial u_{20}}{\partial x_1}\right)^2 + 0 \approx 0 \\
\varepsilon_{23} &\approx 0 \\
\varepsilon_{33} &\approx 0
\end{aligned}
\tag{2}
$$

where $\theta = d\hat{\theta}/dx_1$.
By letting

$$\begin{aligned}
\chi_{22} &= -u_{20,11} \\
\chi_{33} &= -u_{30,11} \\
\varepsilon_{11}^0 &= u_{10,1} + \frac{1}{2}(u_{20,1})^2 + \frac{1}{2}(u_{30,1})^2 = \varepsilon_{11}^{0\mathrm{L}} + \varepsilon_{11}^{0\mathrm{NL}}
\end{aligned} \tag{3}$$

the strain-displacement relations can be rewritten as

$$\begin{aligned}
\varepsilon_{11} &= \varepsilon_{11}^0 + x_2\chi_{22} + x_3\chi_{33} \\
\varepsilon_{12} &= \frac{1}{2}(u_{1T,2} - \theta x_3) \\
\varepsilon_{13} &= \frac{1}{2}(u_{1T,3} + \theta x_2) \\
\varepsilon_{22} &= \varepsilon_{33} = \varepsilon_{23} = 0
\end{aligned} \tag{4}$$

where $,i$ denotes a differentiation with respect to x_i.
The matrix form of the Eq.(4) is

$$\boldsymbol{\varepsilon} = \boldsymbol{\varepsilon}^L + \boldsymbol{\varepsilon}^N \tag{5}$$

where

$$\boldsymbol{\varepsilon}^L = \begin{Bmatrix} \varepsilon_{11}^L \\ \varepsilon_{12}^L \\ \varepsilon_{13}^L \end{Bmatrix} = \begin{Bmatrix} u_{10,1} + x_2\chi_{22} + x_3\chi_{33} \\ \frac{1}{2}(u_{1T,2} - \theta x_3) \\ \frac{1}{2}(u_{1T,3} + \theta x_2) \end{Bmatrix} \tag{6}$$

$$\boldsymbol{\varepsilon}^N = \begin{Bmatrix} \varepsilon_{11}^N \\ \varepsilon_{12}^N \\ \varepsilon_{13}^N \end{Bmatrix} = \begin{Bmatrix} \frac{1}{2}(u_{20,1})^2 + \frac{1}{2}(u_{30,1})^2 \\ 0 \\ 0 \end{Bmatrix} \tag{7}$$

2.2 Stress-Strain relations

Taking the material to be linear elastic, we assume that the additional second Piola-Kirchhoff stress, denoted by tensor $\mathbf{S}^1$ in the updated Lagrangian co-rotational reference frame $\mathbf{e}_i$ of Fig.1 (in addition to the pre-existing Cauchy stress due to prior deformation, denoted by $\boldsymbol{\tau}^0$), is given by:

$$\begin{aligned}
S_{11}^1 &= E\varepsilon_{11} \\
S_{12}^1 &= 2\mu\varepsilon_{12} \\
S_{13}^1 &= 2\mu\varepsilon_{13} \\
S_{22}^1 &= S_{33}^1 = S_{23}^1 \approx 0
\end{aligned} \tag{8}$$

where $\mu = \frac{E}{2(1+\nu)}$; E is the elastic modulus; ν is the Poisson ratio.
By using Eq.(5), Eq.(8) can also be written as

$$\mathbf{S}^1 = \tilde{\mathbf{D}}\left(\boldsymbol{\varepsilon}^L + \boldsymbol{\varepsilon}^N\right) = \mathbf{S}^{1L} + \mathbf{S}^{1N} \tag{9}$$

where

$$\tilde{\mathbf{D}} = \begin{bmatrix} E & 0 & 0 \\ 0 & 2\mu & 0 \\ 0 & 0 & 2\mu \end{bmatrix} \tag{10}$$

From Eq.(4) and Eq.(8), the generalized nodal forces of the rod element in Fig.2 can be written as

$$\begin{aligned}
N_{11} &= \int_A S_{11}^1 dA = E\left(A\varepsilon_{11}^0 + \chi_{22}\int_A x_2 dA + \chi_{33}\int_A x_3 dA\right) \\
&= E\left(A\varepsilon_{11}^0 + I_2\chi_{22} + I_3\chi_{33}\right) \\
M_{33} &= \int_A S_{11}^1 x_3 dA = E\int_A \left(A\varepsilon_{11}^0 + x_2\chi_{22} + x_3\chi_{33}\right)x_3 dA \\
&= E\left(I_3\varepsilon_{11}^0 + I_{23}\chi_{22} + I_{33}\chi_{33}\right) \\
M_{22} &= \int_A S_{11}^1 x_2 dA = E\int_A \left(A\varepsilon_{11}^0 + x_2\chi_{22} + x_3\chi_{33}\right)x_2 dA \\
&= E\left(I_2\varepsilon_{11}^0 + I_{22}\chi_{22} + I_{23}\chi_{33}\right) \\
T &= \int_A S_{13}^1 x_2 - S_{12}^1 x_3 dA = 2\mu\int_A \left(x_2\varepsilon_{13} + x_3\varepsilon_{12}\right)x_2 dA \\
&= \frac{2\mu}{2}\int_A \left[\left(u_{1T,3} + \theta\, x_2\right)x_2 - \left(u_{1T,2} - \theta x_3\right)\right] dA \\
&= \mu\int_A \theta\left(x_2^2 + x_3^2\right) dA + \mu\int_A \left(u_{1T,3}x_2 - u_{1T,2}x_3\right) dA \\
&= \mu I_{rr}\theta + \mu\oint_S \left(u_{1T}n_3x_2 - u_{1T}n_2x_3\right) dS \\
&= \mu I_{rr}\theta
\end{aligned} \tag{11}$$

where n_j is the outward norm, $I_2 = \int_A x_2 dA$, $I_3 = \int_A x_3 dA$, $I_{22} = \int_A x_2^2 dA$, $I_{33} = \int_A x_3^2 dA$, $I_{23} = \int_A x_2 x_3 dA$, and $I_{rr} = \int_A \left(x_2^2 + x_3^2\right) dA$.
The matrix form of the above equations is

$$\begin{Bmatrix} \sigma_1 \\ \sigma_2 \\ \sigma_3 \\ \sigma_4 \end{Bmatrix} = \begin{Bmatrix} N_{11} \\ M_{22} \\ M_{33} \\ T \end{Bmatrix} = \begin{bmatrix} EA & EI_2 & EI_3 & 0 \\ EI_2 & EI_{22} & EI_{23} & 0 \\ EI_3 & EI_{23} & EI_{33} & 0 \\ 0 & 0 & 0 & \mu I_{rr} \end{bmatrix} \begin{Bmatrix} \varepsilon_{11}^0 \\ \chi_{22} \\ \chi_{33} \\ \theta \end{Bmatrix} \tag{12}$$

It can be denoted as

$$\boldsymbol{\sigma} = \mathbf{DE} \tag{13}$$

where

$$\boldsymbol{\sigma} = \begin{Bmatrix} \sigma_1 \\ \sigma_2 \\ \sigma_3 \\ \sigma_4 \end{Bmatrix} = \begin{Bmatrix} N_{11} \\ M_{22} \\ M_{33} \\ T \end{Bmatrix} = \text{element generalized stresses} \tag{14}$$

$$\mathbf{D} = \begin{bmatrix} EA & EI_2 & EI_3 & 0 \\ EI_2 & EI_{22} & EI_{23} & 0 \\ EI_3 & EI_{23} & EI_{33} & 0 \\ 0 & 0 & 0 & \mu I_{rr} \end{bmatrix} \tag{15}$$

$$\mathbf{E} = \mathbf{E}^L + \mathbf{E}^N = \begin{Bmatrix} E_1 \\ E_2 \\ E_3 \\ E_4 \end{Bmatrix} = \begin{Bmatrix} \varepsilon_{11}^0 \\ \chi_{22} \\ \chi_{33} \\ \theta \end{Bmatrix} = \text{element generalized strains} \tag{16}$$

where

$$\mathbf{E}^L = \begin{bmatrix} u_{10,1} & -u_{20,11} & -u_{30,11} & \hat{\theta}_{,1} \end{bmatrix}^T \tag{17}$$

$$\mathbf{E}^N = \begin{bmatrix} \frac{1}{2}\left(u_{20,1}^2 + u_{30,1}^2\right) & 0 & 0 & 0 \end{bmatrix}^T \tag{18}$$

3 Updated Lagrangian formulation in the co-rotational reference frame $\mathbf{e}_i$

3.1 The use of the Reissner variational principle in the co-rotational updated Lagrangian reference frame

If τ_{ij}^0 are the initial Cauchy stresses in the updated Lagrangian co-rotational frame $\mathbf{e}_i$ of Fig.1, $S_{ij}^1$are the additional (incremental) second Piola-Kirchhoff stresses in the same updated Lagrangian co-rotational frame with axes $\mathbf{e}_i$, $S_{ij} = S_{ij}^1 + \tau_{ij}^0$ are the total stresses, and u_i are the incremental displacements in the co-rotational updated-Lagrangian reference frame, the functional of the Reissner variational principle (Reissner 1953) [see also Atluri and Reissner (1989)] for the incremental S_{ij}^1 and u_i in the co-rotational updated Lagrangian reference frame is given by [Atluri 1979, 1980]

$$\Pi_R = \int_V \left\{ -B\left(S_{ij}^1\right) + \frac{1}{2}\tau_{ij}^0 u_{k,i} u_{k,j} + \frac{1}{2} S_{ij}\left(u_{i,j} + u_{j,i}\right) - \rho b_i u_i \right\} dV - \int_{S_\sigma} \bar{T}_i u_i dS \tag{19}$$

Where V is the volume in the current co-rotational reference state, S_σ is the surface where tractions are prescribed, $b_i = b_i^0 + b_i^1$ are the body forces per unit volume in the current reference state, and $\bar{T}_i = \bar{T}_i^0 + \bar{T}_i^1$ are the given boundary tractions.

The conditions of stationarity of Π_R, with respect to variations δS_{ij}^1 and δu_i lead to the following incremental equations in the co-rotational updated- Lagrangian reference frame.

$$\frac{\partial B}{\partial S_{ij}^1} = \frac{1}{2}\left[u_{i,j} + u_{j,i}\right] \tag{20}$$

$$\left[S_{ij}^1 + \tau_{ik}^0 u_{j,k}\right]_{,j} + \rho b_i^1 = -\left(\tau_{ij}^0\right)_{,j} - \rho b_i^0 \tag{21}$$

$$n_j\left[S_{ij}^1 + \tau_{ik}^0 u_{j,k}\right]^- \bar{T}_i^1 = -n_j \tau_{ij}^0 + \bar{T}_i^0 \text{ at } S_\sigma \tag{22}$$

In Eq.(19), the displacement boundary conditions,

$$u_i = \bar{u}_i \text{ at } S_u \tag{23}$$

are assumed to be satisfied a priori, at the external boundary, S_u. Eq.(21) leads to equilibrium correction iterations.

If the variational principle embodied in Eq.(19) is applied to a group of finite elements, V_m, $m = 1, 2, \cdots, N$, which comprise the volume V, ie, $V = \sum V_m$, then

$$\Pi_R = \sum_m \left(\int_{V_m} \left\{ -B\left(S_{ij}^1\right) + \frac{1}{2}\tau_{ij}^0 u_{k,j} u_{k,j} + \frac{1}{2} S_{ij}\left(u_{i,j} + u_{j,i}\right) - \rho b_i u_i \right\} dV - \int_{S_{\sigma m}} \overline{T}_i u_i dS \right) \tag{24}$$

Let ∂V_m be the boundary of V_m, and ρ_m be the part of ∂V_m which is shared by the element with its neighbouring elements. If the trial function u_i and the test function ∂u_i in each V_m are such that the inter-element continuity condition,

$$u_i^+ = u_i^- \text{ at } \rho_m \tag{25}$$

(where + and – refer to either side of the boundary ρ_m) is satisfied a priori, then it can be shown (Atluri 1975,1984; Atluri and Murakawa 1977; Atluri, Gallagher and Zienkiewicz 1983) that the conditions of stationarity of Π_R in Eq.(24) lead to:

$$\frac{\partial B}{\partial S_{ij}^1} = \frac{1}{2}\left[u_{i,j} + u_{j,i}\right] \text{ in } V_m \tag{26}$$

$$\left[S_{ij}^1 + \tau_{ik}^0 u_{j,k}\right]_{,j} + \rho b_i^1 = -\tau_{ij,j}^0 - \rho b_i^0 \text{ in } V_m \tag{27}$$

$$\left[n_i\left(S_{ij}^1 + \tau_{ik}^0 u_{j,k}\right)\right]^+ + \left[n_i\left(S_{ij}^1 + \tau_{ik}^0 u_{j,k}\right)\right]^- = -\left[n_i\tau_{ij}^0\right]^+ - \left[n_i\tau_{ij}^0\right]^- \text{ at } \rho_m \tag{28}$$

$$n_j\left[S_{ij}^1 + \tau_{ik}^0 u_{j,k}\right] - \bar{T}_i^1 = -n_j\tau_{ij}^0 + \bar{T}_i^0 \text{ at } S_{\sigma\mathrm{m}} \tag{29}$$

Eq.(28) is the condition of traction reciprocity at the inter-element boundary, ρ_m. Eqs(27) and (28) lead to corrective iterations for equilibrium within each element, and traction reciprocity at the inter-element boundaries, respectively.

Carrying out the integration over the cross sectional area of each rod, and using Eqs.(4) and (12), Eq.(24) can be easily shown to reduce to:

$$\begin{aligned}\Pi_R = \sum_{elem}\Bigg\{ &\int_l \left(-\frac{1}{2}\boldsymbol{\sigma}^T\mathbf{D}^{-1}\boldsymbol{\sigma}\right) dl + \int_l N_{11}^0 \frac{1}{2}\left(u_{20,1}^2 + u_{30,1}^2\right) dl \\ &+ \int_l \left(\hat{N}_{11}\varepsilon_{11}^{0\mathrm{L}} + \hat{M}_{22}\chi_{22} + \hat{M}_{33}\chi_{33} + \hat{T}\theta\right) dl - \bar{\mathbf{Q}}\mathbf{q}\Bigg\}\end{aligned} \tag{30}$$

where $\mathbf{D}$ is given in Eq.(15), $\mathbf{C} = \mathbf{D}^{-1}$, l is the length of the rod element, $\boldsymbol{\sigma}$ is given in Eq.(14), $\sigma_{ij}^0 = \begin{bmatrix} N_{11}^0 & M_{22}^0 & M_{33}^0 & T^0 \end{bmatrix}^T$ is the initial element-generalized- stress in the corotational reference coordinates $\mathbf{e}_i$, and $\hat{\boldsymbol{\sigma}} = \boldsymbol{\sigma}^0 + \boldsymbol{\sigma} = \begin{bmatrix} \hat{N}_{11} & \hat{M}_{22} & \hat{M}_{33} & \hat{T} \end{bmatrix}^T$ is the total element generalized stresses in the corotational reference coordinates $\mathbf{e}_i$. $\bar{\mathbf{Q}}$ is the nodal external generalized force vector (consisting of force as well as moments) in the global Cartesian reference frame, and $\mathbf{q}$ is the incremental nodal generalized displacement vector (consisting of displacements as well as rotations) in the global Cartesian reference frame. It should be noted that while Π_R in Eq.(30) represents a sum over the elements, the relevant integrals are evaluated over each element in it's own co-rotational updated Lagrangian reference frame.

By integrating by parts, the second item of the left side can be written as

$$\begin{aligned}
\int_l \hat{N}_{11}\varepsilon_{11}^{0\mathrm{L}}dl &= \int_l \hat{N}_{11}u_{10,1}dl = -\int_l \hat{N}_{11,1}u_{10}dl + \hat{N}_{11}u_{10}\big|_0^l \\
\int_l \hat{M}_{22}\chi_{22}dl &= -\int_l \hat{M}_{22}u_{20,11}dl \\
&= -\int_l \hat{M}_{22,11}u_{20}dl + \hat{M}_{22,1}u_{20}\big|_0^l - \hat{M}_{22}u_{20,1}\big|_0^l \\
\int_l \hat{M}_{33}\chi_{33}dl &= -\int_l \hat{M}_{33}u_{30,11}dl \\
&= -\int_l \hat{M}_{33,11}u_{30}dl + \hat{M}_{33,1}u_{30}\big|_0^l - \hat{M}_{33}u_{30,1}\big|_0^l \\
\int_l \hat{T}\theta dl &= \int_l \hat{T}\hat{\theta}_{,1}dl = -\int_l \hat{T}_{,1}\hat{\theta}dl + \hat{T}\hat{\theta}\big|_0^l
\end{aligned} \tag{31}$$

The condition of stationarity of Π_R in Eq.(30) leads to:

$$\begin{aligned}
&\mathrm{D}^{-1}\boldsymbol{\sigma} = E = \begin{bmatrix} u_{10,1} & -u_{20,11} & -u_{30,11} & \theta \end{bmatrix}^T \\
&\hat{N}_{11,1} = 0 \text{ in each element} \\
&\hat{T}_{,1} = 0 \text{ in each element} \\
&\hat{M}_{22,11} + \left(N_{11}^0 u_{20,1}\right)_{,1} = 0 \text{ in each element} \\
&\hat{M}_{33,11} + \left(N_{11}^0 u_{30,1}\right)_{,1} = 0 \text{ in each element}
\end{aligned} \tag{32}$$

and the nodal equilibrium equations, which arise out of the term:

$$\begin{aligned}
\sum_{elem} \Big(&\hat{N}_{11}\delta u_{10}\big|_0^l + \hat{M}_{22,1}\delta u_{20}\big|_0^l - \hat{M}_{22}\delta u_{20,1}\big|_0^l + \hat{M}_{33,1}\delta u_{30}\big|_0^l - \hat{M}_{33}\delta u_{30,1}\big|_0^l + \\
&\hat{T}\delta\hat{\theta}\big|_0^l + \left(N_{11}^0 u_{20,1}\right)\delta u_{20}\big|_0^l + \left(N_{11}^0 u_{30,1}\right)\delta u_{30}\big|_0^l - \bar{\mathbf{Q}}\delta\mathbf{q}\Big) = 0
\end{aligned} \tag{33}$$

3.2 Trial functions of the stresses and displacements in each element

We assume the trial functions for N_{11}, M_{22}, M_{33} and T, in each element, as

$$\begin{aligned} N_{11} &= n \\ M_{22} &= -m_3 = -\left(1-\frac{x_1}{l}\right){}^1m_3 - \frac{x_1}{l}{}^2m_3 \\ M_{33} &= m_2 = \left(1-\frac{x_1}{l}\right){}^1m_2 + \frac{x_1}{l}{}^2m_2 \\ T &= m_1 \end{aligned} \tag{34}$$

The matrix form of the above equation is

$$\boldsymbol{\sigma} = \mathbf{P}\boldsymbol{\beta} \tag{35}$$

where

$$\mathbf{P} = \begin{bmatrix} 1 & 0 & 0 & 0 & 0 & 0 \\ 0 & -1+\frac{x_1}{l} & -\frac{x_1}{l} & 0 & 0 & 0 \\ 0 & 0 & 0 & 1-\frac{x_1}{l} & \frac{x_1}{l} & 0 \\ 0 & 0 & 0 & 0 & 0 & 1 \end{bmatrix} \tag{36}$$

$$\boldsymbol{\beta} = \begin{bmatrix} n & {}^1m_3 & {}^2m_3 & {}^1m_2 & {}^2m_2 & m_1 \end{bmatrix}^T \tag{37}$$

In a same way, the initial stress $\boldsymbol{\sigma}^0$ can be expressed as

$$\boldsymbol{\sigma}^0 = \mathbf{P}\boldsymbol{\beta}^0 \tag{38}$$

where

$$\boldsymbol{\beta}^0 = \begin{bmatrix} n^0 & {}^1m_3^0 & {}^2m_3^0 & {}^1m_2^0 & {}^2m_2^0 & m_1^0 \end{bmatrix}^T \tag{39}$$

The incremental internal nodal force vector $\boldsymbol{\beta}_n$ of node 1 and node 2 of a rod

$$\boldsymbol{\beta}_n = \begin{bmatrix} {}^1N & {}^1m_1 & {}^1m_2 & {}^1m_3 & {}^2N & {}^2m_1 & {}^2m_2 & {}^2m_3 \end{bmatrix}^T$$

can be expressed as

$$\boldsymbol{\beta}_n = \mathbf{R}_n\boldsymbol{\beta} \tag{40}$$

where

$$\mathbf{R}_n = \begin{bmatrix} 1 & 0 & 0 & 0 & 0 & 0 \\ 0 & 0 & 0 & 0 & 0 & 1 \\ 0 & 0 & 0 & 1 & 0 & 0 \\ 0 & 1 & 0 & 0 & 0 & 0 \\ 1 & 0 & 0 & 0 & 0 & 0 \\ 0 & 0 & 0 & 0 & 0 & 1 \\ 0 & 0 & 0 & 0 & 1 & 0 \\ 0 & 0 & 1 & 0 & 0 & 0 \end{bmatrix} \tag{41}$$

In the functional in Eq.(30), only the squares of $(u_{20,1})$ and $(u_{30,1})$ occur within each element. Thus, $(u_{20,1})$ and $(u_{30,1})$ are assumed directly to be linear within each element, in terms of their respective nodal values. This will be enormously simple and advantageous in the case of plate and shell elements. This is in contrast to the primal (displacement) approach (Cai, Paik and Atluri 2010) wherein u_{20} and u_{30} were required to be C^1 continuous over each element, and thus were assumed to be Herimitian polynomials over each element. In this paper, however, we assume:

$$\mathbf{u}_\theta = \mathbf{N}_\theta \mathbf{a}_\theta = \begin{bmatrix} \phi_1 & 0 & \phi_2 & 0 \\ 0 & \phi_1 & 0 & \phi_2 \end{bmatrix} \begin{Bmatrix} {}^1\theta_{20} \\ {}^1\theta_{30} \\ {}^2\theta_{20} \\ {}^2\theta_{30} \end{Bmatrix} \tag{42}$$

where

$$\begin{aligned} &\phi_1 = 1 - \xi \\ &\phi_2 = \xi \end{aligned} \qquad \left(\xi = \frac{x_1}{l}\right) \tag{43}$$

Assuming that '**a**' represents the vector of generalized displacements of the nodes of the rod element in the updated Lagrangian co-rotational frame $\mathbf{e}_i$ of Fig.1, the displacement vectors of node i are:

$$\begin{aligned} {}^i\mathbf{a} &= \begin{bmatrix} {}^iu_1 & {}^iu_2 & {}^iu_3 & {}^iu_4 & {}^iu_5 & {}^iu_6 \end{bmatrix}^T \\ &= \begin{bmatrix} {}^iu_{10} & {}^iu_{20} & {}^iu_{30} & {}^i\hat{\theta} & {}^i\theta_{20} & {}^i\theta_{30} \end{bmatrix}^T \quad (i = 1,2) \end{aligned} \tag{44}$$

The relation between $\mathbf{a}_\theta$ and $\mathbf{a}$ can be expressed as

$$\mathbf{a}_\theta = \mathbf{T}_\theta \mathbf{a} \tag{45}$$

where

$$\mathbf{T}_\theta = \begin{bmatrix} 0 & 0 & 0 & 0 & 1 & 0 & 0 & 0 & 0 & 0 & 0 & 0 \\ 0 & 0 & 0 & 0 & 0 & 1 & 0 & 0 & 0 & 0 & 0 & 0 \\ 0 & 0 & 0 & 0 & 0 & 0 & 0 & 0 & 0 & 0 & 1 & 0 \\ 0 & 0 & 0 & 0 & 0 & 0 & 0 & 0 & 0 & 0 & 0 & 1 \end{bmatrix} \tag{46}$$

3.3 Explicit expressions of the tangent stiffness matrix for each element

Because of the assumption of the trial functions of the stresses in Eqs.(35), the following items in Eq.(31) become

$$\begin{aligned}
&\int_l \hat{N}_{11,1} u_{10} dl = 0 \\
&\int_l \hat{M}_{22,11} u_{20} dl = 0 \\
&\int_l \hat{M}_{33,11} u_{30} dl = 0 \\
&\int_l \hat{T}_{,1} \hat{\theta} dl = 0
\end{aligned} \tag{47}$$

Eq.(30) can be rewritten as

$$\Pi_R = -\Pi_{R1} + \Pi_{R2} + \Pi_{R3} - \Pi_{R4} \tag{48}$$

where

$$\Pi_{R1} = \sum_{elem} \int_l \left(\frac{1}{2} \boldsymbol{\sigma}^T \mathbf{D}^{-1} \boldsymbol{\sigma} \right) dl = \sum_{elem} \int_l \left(\frac{1}{2} \boldsymbol{\beta}^T \mathbf{P}^T \mathbf{C} \mathbf{P} \boldsymbol{\beta} \right) dl \tag{49}$$

$$\begin{aligned}
\Pi_{R2} = \sum_{elem} \Big\{ & {}^2N^2 u_{10} - {}^1N^1 u_{10} + \frac{1}{l} \left({}^1m_3 - {}^2m_3 \right) \left({}^2u_{20} - {}^1u_{20} \right) + {}^2m_3{}^2\theta_{30} - {}^1m_3{}^1\theta_{30} \\
& + \frac{1}{l} \left({}^2m_2 - {}^1m_2 \right) \left({}^2u_{30} - {}^1u_{30} \right) + {}^2m_2{}^2\theta_{20} - {}^1m_2{}^1\theta_{20} + {}^2m_1{}^2\hat{\theta} - {}^1m_1{}^1\hat{\theta} \Big\} \\
= & \sum_{elem} \left\{ (\boldsymbol{\beta}_n)^T \mathbf{R}_\sigma \mathbf{a} \right\} = \sum_{elem} \left\{ (\boldsymbol{\beta})^T \mathbf{R}_n^T \mathbf{R}_\sigma \mathbf{a} \right\}
\end{aligned} \tag{50}$$

where

$$\mathbf{R}_\sigma = \begin{bmatrix}
-1 & 0 & 0 & 0 & 0 & 0 & 0 & 0 & 0 & 0 & 0 & 0 \\
0 & 0 & 0 & -1 & 0 & 0 & 0 & 0 & 0 & 0 & 0 & 0 \\
0 & 0 & \frac{1}{l} & 0 & -1 & 0 & 0 & 0 & -\frac{1}{l} & 0 & 0 & 0 \\
0 & -\frac{1}{l} & 0 & 0 & 0 & -1 & 0 & \frac{1}{l} & 0 & 0 & 0 & 0 \\
0 & 0 & 0 & 0 & 0 & 0 & 1 & 0 & 0 & 0 & 0 & 0 \\
0 & 0 & 0 & 0 & 0 & 0 & 0 & 0 & 0 & 1 & 0 & 0 \\
0 & 0 & -\frac{1}{l} & 0 & 0 & 0 & 0 & 0 & \frac{1}{l} & 0 & 1 & 0 \\
0 & \frac{1}{l} & 0 & 0 & 0 & 0 & 0 & -\frac{1}{l} & 0 & 0 & 0 & 1
\end{bmatrix} \tag{51}$$

$$\Pi_{R3} = \sum_{elem} \int_l N_{11}^0 \left[\frac{1}{2} (u_{20,1})^2 + \frac{1}{2} (u_{30,1})^2 \right] dl = \sum_{elem} \int_l \sigma_1^0 \left[\frac{1}{2} (\theta_{20})^2 + \frac{1}{2} (\theta_{30})^2 \right] dl$$
$$= \sum_{elem} \int_l \frac{\sigma_1^0}{2} \mathbf{u}_\theta^T \mathbf{u}_\theta dl = \sum_{elem} \int_l \frac{\sigma_1^0}{2} \mathbf{a}^T \mathbf{T}_\theta^T \mathbf{N}_\theta^T \mathbf{N}_\theta \mathbf{T}_\theta \mathbf{a} dl \tag{52}$$

Letting $\mathbf{A}_{nn} = \mathbf{T}_\theta^T \mathbf{N}_\theta^T \mathbf{N}_\theta \mathbf{T}_\theta$, Π_{R3} can be rewritten as

$$\Pi_{R3} = \sum_{elem} \int_l \frac{\sigma_1^0}{2} \mathbf{a}^T \mathbf{A}_{nn} \mathbf{a} dl \tag{53}$$

and

$$\Pi_{R4} = \sum_{elem} \left(\mathbf{a}^T \mathbf{F} - \mathbf{a}^T \mathbf{R}_\sigma^T \mathbf{R}_n \boldsymbol{\beta}^0 \right) \tag{54}$$

By invoking $\delta \Pi_R = 0$, we can obtain

$$\delta \Pi_R = \sum_{elem} \delta \boldsymbol{\beta}^T \left\{ - \int_l \mathbf{P}^T \mathbf{C} \mathbf{P} \beta dl + \mathbf{R}_n^T \mathbf{R}_\sigma \mathbf{a} \right\} +$$
$$\sum_{elem} \delta \mathbf{a}^T \left\{ \mathbf{R}_\sigma^T \mathbf{R}_n \boldsymbol{\beta} + \sigma_1^0 \int_l \mathbf{A}_{nn} \mathbf{a} dl + \mathbf{R}_\sigma^T \mathbf{R}_n \boldsymbol{\beta}^0 - \mathbf{F} \right\} \tag{55}$$

Let

$$\mathbf{H} = \int_l \mathbf{P}^T \mathbf{C} \mathbf{P} dl, \quad \mathbf{G} = \mathbf{R}_n^T \mathbf{R}_\sigma, \quad \mathbf{K}_N = \sigma_1^0 \int_l \mathbf{A}_{nn} dl, \quad \mathbf{F}^0 = \mathbf{G}^T \boldsymbol{\beta}^0 \tag{56}$$

then

$$\delta \Pi_R = \sum_{elem} \delta \boldsymbol{\beta}^T \left\{ -\mathbf{H} \beta + \mathbf{G} \mathbf{a} \right\} - \sum_{elem} \delta \mathbf{a}^T \left\{ \mathbf{G}^T \boldsymbol{\beta} + \mathbf{K}_N \mathbf{a} - \mathbf{F} + \mathbf{F}^0 \right\} = 0 \tag{57}$$

Since $\delta \boldsymbol{\beta}^T$ in Eq.(53) are independent and arbitrary in each element, one obtains

$$\boldsymbol{\beta} = \mathbf{H}^{-1} \mathbf{G} \mathbf{a} \tag{58}$$

and

$$\sum_{elem} \delta \mathbf{a}^T \left\{ (\mathbf{K}_L + \mathbf{K}_N) \mathbf{a} - \mathbf{F} + \mathbf{F}^0 \right\} = 0 \tag{59}$$

where

$$\mathbf{K}_L = \mathbf{G}^{\mathbf{T}}\mathbf{H}^{-1}\mathbf{G} \tag{60}$$

$$\mathbf{K}_N = \sigma_1^0 \int_l \mathbf{A}_{nn} dl \tag{61}$$

The components of the element tangent stiffness matrix, $\mathbf{K}_L$ and $\mathbf{K}_N$, respectively, can be derived explicitly, after some simple algebra, as follows.

$$\mathbf{K}_N = \frac{l\sigma_1^0}{6}\begin{bmatrix} 0 & 0 & 0 & 0 & 0 & 0 & 0 & 0 & 0 & 0 & 0 & 0 \\ & 0 & 0 & 0 & 0 & 0 & 0 & 0 & 0 & 0 & 0 & 0 \\ & & 0 & 0 & 0 & 0 & 0 & 0 & 0 & 0 & 0 & 0 \\ & & & 0 & 0 & 0 & 0 & 0 & 0 & 0 & 0 & 0 \\ & & & & 2 & 0 & 0 & 0 & 0 & 0 & 1 & 0 \\ & & & & & 2 & 0 & 0 & 0 & 0 & 0 & 1 \\ & & & & & & 0 & 0 & 0 & 0 & 0 & 0 \\ & & & & & & & 0 & 0 & 0 & 0 & 0 \\ & & & sym. & & & & & 0 & 0 & 0 & 0 \\ & & & & & & & & & 0 & 0 & 0 \\ & & & & & & & & & & 2 & 0 \\ & & & & & & & & & & & 2 \end{bmatrix} \tag{62}$$

$$\mathbf{K}_L = \frac{E}{lA}\begin{bmatrix} \mathbf{K}_{L1} & \mathbf{K}_{L12} \\ \mathbf{K}_{L12}^T & \mathbf{K}_{L2} \end{bmatrix} \tag{63}$$

where

$$\mathbf{K}_{L1} = \begin{bmatrix} A^2 & 0 & 0 & 0 & AI_3 & -AI_2 \\ & \frac{12\left(AI_{22}-I_2^2\right)}{l^2} & \frac{12(AI_{23}-I_2I_3)}{l^2} & 0 & \frac{-6(AI_{23}-I_2I_3)}{l} & \frac{6\left(AI_{22}-I_2^2\right)}{l} \\ & & \frac{12\left(AI_{33}-I_3^2\right)}{l^2} & 0 & \frac{-6\left(AI_{33}-I_3^2\right)}{l} & \frac{6(AI_{23}-I_2I_3)}{l} \\ & & & \frac{A\mu}{E}I_{rr} & 0 & 0 \\ & \text{symmetric} & & & 4AI_{33}-3I_3^2 & -4AI_{23}+3I_2I_3 \\ & & & & & 4AI_{22}-3I_2^2 \end{bmatrix} \tag{64}$$

$$\mathbf{K}_{L2} = \begin{bmatrix} A^2 & 0 & 0 & 0 & AI_3 & -AI_2 \\ & \frac{12\left(AI_{22}-I_2^2\right)}{l^2} & \frac{12(AI_{23}-I_2I_3)}{l^2} & 0 & \frac{6(AI_{23}-I_2I_3)}{l} & \frac{-6\left(AI_{22}-I_2^2\right)}{l} \\ & & \frac{12\left(AI_{33}-I_3^2\right)}{l^2} & 0 & \frac{6\left(AI_{33}-I_3^2\right)}{l} & \frac{-6(AI_{23}-I_2I_3)}{l} \\ & & & \frac{A\mu}{E}I_{rr} & 0 & 0 \\ & \text{symmetric} & & & 4AI_{33}-3I_3^2 & -4AI_{23}+3I_2I_3 \\ & & & & & 4AI_{22}-3I_2^2 \end{bmatrix} \tag{65}$$

$$\mathbf{K}_{L12} = \begin{bmatrix} -A^2 & 0 & 0 & 0 & -AI_3 & AI_2 \\ 0 & \frac{-12\left(AI_{22}-I_2^2\right)}{l^2} & \frac{-12(AI_{23}-I_2I_3)}{l^2} & 0 & \frac{-6(AI_{23}-I_2I_3)}{l} & \frac{6\left(AI_{22}-I_2^2\right)}{l} \\ 0 & \frac{-12(AI_{23}-I_2I_3)}{l^2} & \frac{-12\left(AI_{33}-I_3^2\right)}{l^2} & 0 & \frac{-6\left(AI_{33}-I_3^2\right)}{l} & \frac{6(AI_{23}-I_2I_3)}{l} \\ 0 & 0 & 0 & -\frac{A\mu}{E}I_{rr} & 0 & 0 \\ -AI_3 & \frac{6(AI_{23}-I_2I_3)}{l} & \frac{6\left(AI_{33}-I_3^2\right)}{l} & 0 & 2AI_{33}-3I_3^2 & -2AI_{23}+3I_2I_3 \\ AI_2 & \frac{-6\left(AI_{22}-I_2^2\right)}{l} & \frac{-6(AI_{23}-I_2I_3)}{l} & 0 & -2AI_{23}+3I_2I_3 & 2AI_{22}-3I_2^2 \end{bmatrix} \tag{66}$$

Thus, $\mathbf{K}_L$ is the usual linear symmetric (12×12) stiffness matrix of the beam in the co-rotational reference frame, with the geometric parameters I_2, I_3, I_{22}, I_{33}, I_{23} and I_{rr}, and the current length l.

It is clear from the above procedures, that the present (12×12) symmetric tangent stiffness matrices of the beam in the co-rotational reference frame, based on the Reissner variational principle and simplified rod theory, are much simpler than those of Kondon, Tanaka and Atluri (1986), Kondoh and Atluri (1987), and Shi and Atluri (1988). Moreover, the explicit expressions for the tangent stiffness matrix of each rod can be seen to be derived as text-book examples of nonlinear analyses.

3.4 Cubic trial functions of the displacements in the beam element, using the Reissner variational principle

When using the Reissner functional in Eq.(30), one may directly assume the rotation field $(u_{20,1})$ and $(u_{30,1})$ as linear functions in terms only of their respective nodal values, as in Eq.(42). Alternatively, u_{20} and u_{30} may be assumed as cubic polynomials in terms of the four nodal values ${}^1u_{20}$, ${}^2u_{20}$, ${}^1u_{20,1}$, ${}^2u_{20,1}$ (${}^1u_{30}$, ${}^2u_{30}$, ${}^1u_{30,1}$, ${}^2u_{30,1}$ for u_{30}), and derive the element fields for $u_{20,1}$ (and $u_{30,1}$) from these cubic polynomials [even though the Reissner principle does not demand it]. This will be particularly advantageous for plate and shell elements which demand C^1

continuity while using the potential energy approach, while C^1 continuity of the displacement field will not be demanded in the Reissner principle.

In general, we assume over each element:

$$\begin{aligned} u_{20} &= \alpha_1 + \alpha_2\xi + \alpha_3\xi^2 + \alpha_4\xi^3 \\ u_{30} &= \gamma_1 + \gamma_2\xi + \gamma_3\xi^2 + \gamma_4\xi^3 \end{aligned} \tag{67}$$

By letting

$$\begin{aligned} &u_{20}|_{\xi=\xi_0} = {}^1u_{20},\ u_{20}|_{\xi=\xi_1} = {}^2u_{20},\ u_{20,1}|_{\xi=\xi_0} = {}^1\theta_{30},\ u_{20,1}|_{\xi=\xi_1} = {}^2\theta_{30} \\ &u_{30}|_{\xi=\xi_0} = {}^1u_{30},\ u_{30}|_{\xi=\xi_1} = {}^2u_{30},\ -u_{30,1}|_{\xi=\xi_0} = {}^1\theta_{20},\ -u_{30,1}|_{\xi=\xi_1} = {}^2\theta_{20} \end{aligned} \tag{68}$$

we can approximate the displacement function in each rod element by

$$\mathbf{u}_c = \mathbf{N}\mathbf{a} = \begin{bmatrix} {}^1\mathbf{N} & {}^2\mathbf{N} \end{bmatrix} \begin{Bmatrix} {}^1\mathbf{a} \\ {}^2\mathbf{a} \end{Bmatrix} \tag{69}$$

where

$$\mathbf{u}_c = \begin{bmatrix} u_{10} & u_{20} & u_{30} & \hat{\theta} \end{bmatrix}^T \tag{70}$$

$${}^1\mathbf{N} = \begin{bmatrix} \phi_1 & 0 & 0 & 0 & 0 & 0 \\ 0 & N_1 & 0 & 0 & 0 & N_2 \\ 0 & 0 & N_1 & 0 & -N_2 & 0 \\ 0 & 0 & 0 & \phi_1 & 0 & 0 \end{bmatrix} \tag{71}$$

$${}^1\mathbf{N} = \begin{bmatrix} \phi_2 & 0 & 0 & 0 & 0 & 0 \\ 0 & N_3 & 0 & 0 & 0 & N_4 \\ 0 & 0 & N_3 & 0 & -N_4 & 0 \\ 0 & 0 & 0 & \phi_2 & 0 & 0 \end{bmatrix} \tag{72}$$

$$\begin{aligned} N_1 &= 1 - 3\xi^2 + 2\xi^3, N_3 = 3\xi^2 - 2\xi^3 \\ N_2 &= \left(\xi - 2\xi^2 + \xi^3\right) l, N_4 = \left(\xi^3 - \xi^2\right) l \end{aligned} \tag{73}$$

and ϕ_1, ϕ_2 are defined in Eq.(43).

By using the cubic trial functions of Eq.(69) and deriving the equations in a same way as the section 3.3, we obtain the respective discrete equations, as follows.

$$\sum_{elem} \delta\mathbf{a}^T \left\{ \left(\mathbf{K}_L + \mathbf{K}_N^c\right)\mathbf{a} - \mathbf{F} + \mathbf{F}^0 \right\} = 0 \tag{74}$$

where $\mathbf{K}_L, \mathbf{F}$ and $\mathbf{F}^0$ are the same as Eq.(59), and the nonlinear stiffness matrix $\mathbf{K}_N^c$ is explicitly expressed as

$$\mathbf{K}_N^c = \frac{\sigma_1^0}{l} \underbrace{\begin{bmatrix} 0 & 0 & 0 & 0 & 0 & 0 & 0 & 0 & 0 & 0 & 0 & 0 \\ & 1.2 & 0 & 0 & 0 & 0.1l & 0 & -1.2 & 0 & 0 & 0 & 0.1l \\ & & 1.2 & 0 & -0.1l & 0 & 0 & 0 & -1.2 & 0 & -0.1l & 0 \\ & & & 0 & 0 & 0 & 0 & 0 & 0 & 0 & 0 & 0 \\ & & & & \frac{2l^2}{15} & 0 & 0 & 0 & 0.1l & 0 & \frac{-l^2}{30} & 0 \\ & & & & & \frac{2l^2}{15} & 0 & -0.1l & 0 & 0 & 0 & \frac{-l^2}{30} \\ & & & & & & 0 & 0 & 0 & 0 & 0 & 0 \\ & & & & & & & 1.2 & 0 & 0 & 0 & -0.1l \\ & & & & sym. & & & & 1.2 & 0 & 0.1l & 0 \\ & & & & & & & & & 0 & 0 & 0 \\ & & & & & & & & & & \frac{2l^2}{15} & 0 \\ & & & & & & & & & & & \frac{2l^2}{15} \end{bmatrix}}_{(12\times 12 \text{ symmetric matrix})} \tag{75}$$

4 Transformation between deformation dependent co-rotational local $[\mathbf{e}_i]$, and the global $[\bar{\mathbf{e}}_i]$ frames of reference

As shown in Fig.1, $\bar{x}_i\,(i=1,2,3)$ are the global coordinates with unit basis vectors $\bar{\mathbf{e}}_i$. $\tilde{x}_i$ and $\tilde{\mathbf{e}}_i$ are the local coordinates for the rod element at the undeformed element. The basis vector $\tilde{\mathbf{e}}_i$ are initially chosen such that (Shi and Atluri 1988, Cai, Paik and Atluri 2010)

$$\begin{aligned} \tilde{\mathbf{e}}_1 &= (\Delta\tilde{x}_1\bar{\mathbf{e}}_1 + \Delta\tilde{x}_2\bar{\mathbf{e}}_2 + \Delta\tilde{x}_3\bar{\mathbf{e}}_3)/L \\ \tilde{\mathbf{e}}_2 &= (\bar{\mathbf{e}}_3 \times \tilde{\mathbf{e}}_1)/|\bar{\mathbf{e}}_3 \times \tilde{\mathbf{e}}_1| \\ \tilde{\mathbf{e}}_3 &= \tilde{\mathbf{e}}_1 \times \tilde{\mathbf{e}}_2 \end{aligned} \tag{76}$$

where $\Delta\tilde{x}_i = \tilde{x}_i^2 - \tilde{x}_i^1, L = \left(\Delta\tilde{x}_1^2 + \Delta\tilde{x}_2^2 + \Delta\tilde{x}_3^2\right)^{\frac{1}{2}}$.
Then $\tilde{\mathbf{e}}_i$ and $\bar{\mathbf{e}}_i$ have the following relations:

$$\begin{Bmatrix} \tilde{\mathbf{e}}_1 \\ \tilde{\mathbf{e}}_2 \\ \tilde{\mathbf{e}}_3 \end{Bmatrix} = \begin{bmatrix} \Delta\tilde{x}_1/L & \Delta\tilde{x}_2/L & \Delta\tilde{x}_3/L \\ -\Delta\tilde{x}_2/S & \Delta\tilde{x}_1/S & 0 \\ -\Delta\tilde{x}_1\Delta\tilde{x}_3/(SL) & -\Delta\tilde{x}_2\Delta\tilde{x}_3/(SL) & s/L \end{bmatrix} \begin{Bmatrix} \bar{\mathbf{e}}_1 \\ \bar{\mathbf{e}}_2 \\ \bar{\mathbf{e}}_3 \end{Bmatrix} \tag{77}$$

where $S = \left(\Delta\tilde{x}_1^2 + \Delta\tilde{x}_2^2\right)^{\frac{1}{2}}$.

Thus we can define a transformation matrix $\tilde{\boldsymbol{\lambda}}_0$ between $\tilde{\mathbf{e}}_i$ and $\bar{\mathbf{e}}_i$ as

$$\tilde{\boldsymbol{\lambda}}_0 = \begin{bmatrix} \Delta\tilde{x}_1/L & \Delta\tilde{x}_2/L & \Delta\tilde{x}_3/L \\ -\Delta\tilde{x}_2/S & \Delta\tilde{x}_1/S & 0 \\ -\Delta\tilde{x}_1\Delta\tilde{x}_3/(SL) & -\Delta\tilde{x}_2\Delta\tilde{x}_3/(SL) & S/L \end{bmatrix} \tag{78}$$

When the element is parallel to the $\bar{x}_3$ axis, $S = \left[\Delta\tilde{x}_1^2 + \Delta\tilde{x}_2^2\right]^{\frac{1}{2}} = 0$ and Eq.(64) is not valid. In this case, the local coordinates is determined by

$$\tilde{\mathbf{e}}_1 = \bar{\mathbf{e}}_3, \tilde{\mathbf{e}}_2 = \bar{\mathbf{e}}_2, \tilde{\mathbf{e}}_3 = -\bar{\mathbf{e}}_1 \tag{79}$$

Let x_i and $\mathbf{e}_i$ be the co-rotational reference coordinates for the deformed rod element. In order to continuously define the local coordinates of the same rod element during the whole range of large deformation, the basis vectors $\mathbf{e}_i$ are chosen such that

$$\begin{aligned} \mathbf{e}_1 &= (\Delta x_1\bar{\mathbf{e}}_1 + \Delta x_2\bar{\mathbf{e}}_2 + \Delta x_3\bar{\mathbf{e}}_3)/l = a_1\bar{\mathbf{e}}_1 + a_2\bar{\mathbf{e}}_2 + a_3\bar{\mathbf{e}}_3 \\ \mathbf{e}_2 &= (\tilde{\mathbf{e}}_3 \times \mathbf{e}_1)/|\tilde{\mathbf{e}}_3 \times \mathbf{e}_1| \\ \mathbf{e}_3 &= \mathbf{e}_1 \times \mathbf{e}_2 \end{aligned} \tag{80}$$

where $\Delta x_i = x_i^2 - x_i^1, l = \left(\Delta x_1^2 + \Delta x_2^2 + \Delta x_3^2\right)^{\frac{1}{2}}$.
We denote $\tilde{\mathbf{e}}_3$ in Eq.(77) as

$$\tilde{\mathbf{e}}_3 = c_1\bar{\mathbf{e}}_1 + c_2\bar{\mathbf{e}}_2 + c_3\bar{\mathbf{e}}_3 \tag{81}$$

Then $\mathbf{e}_i$ and $\bar{\mathbf{e}}_i$ have the following relations:

$$\begin{Bmatrix} \mathbf{e}_1 \\ \mathbf{e}_2 \\ \mathbf{e}_3 \end{Bmatrix} = \begin{bmatrix} a_1 & a_2 & a_3 \\ b_1 & b_2 & b_3 \\ a_2b_3 - a_3b_2 & a_3b_1 - a_1b_3 & a_1b_2 - a_2b_1 \end{bmatrix} \begin{Bmatrix} \bar{\mathbf{e}}_1 \\ \bar{\mathbf{e}}_2 \\ \bar{\mathbf{e}}_3 \end{Bmatrix} = \boldsymbol{\lambda}_0\bar{\mathbf{e}}_i \tag{82}$$

where

$$\begin{aligned} b_1 &= (c_2a_3 - c_3a_2)/l_{31} \\ b_2 &= (c_3a_1 - c_1a_3)/l_{31} \\ b_3 &= (c_1a_2 - c_2a_1)/l_{31} \end{aligned} \tag{83}$$

$$l_{31} = \left[(c_2a_3 - c_3a_2)^2 + (c_3a_1 - c_1a_3)^2 + (c_1a_2 - c_2a_1)^2\right]^{\frac{1}{2}} \tag{84}$$

and

$$\boldsymbol{\lambda}_0 = \begin{bmatrix} a_1 & a_2 & a_3 \\ b_1 & b_2 & b_3 \\ a_2b_3 - a_3b_2 & a_3b_1 - a_1b_3 & a_1b_2 - a_2b_1 \end{bmatrix} \tag{85}$$

Thus, the transformation matrix $\boldsymbol{\lambda}$, between the 12 generalized coordinates in the co-rotational reference frame, and the corresponding 12 coordinates in the global Cartesian reference frame, is given by

$$\boldsymbol{\lambda} = \begin{bmatrix} \boldsymbol{\lambda}_0 & & & \\ & \boldsymbol{\lambda}_0 & & \\ & & \boldsymbol{\lambda}_0 & \\ & & & \boldsymbol{\lambda}_0 \end{bmatrix} \tag{86}$$

Letting x_i and $\mathbf{e}_i$ be the reference coordinates, and repeating the above steps [Eq.(70) – Eq.(86)], the transformation matrix of each incremental step can be obtained in a same way.

Then the element matrices are transformed to the global coordinate system using

$$\bar{\mathbf{a}} = \boldsymbol{\lambda}^T \mathbf{a} \tag{87}$$

$$\bar{\mathbf{K}} = \boldsymbol{\lambda}^T \mathbf{K} \boldsymbol{\lambda} \tag{88}$$

$$\bar{\mathbf{F}} = \boldsymbol{\lambda}^T \mathbf{F} \tag{89}$$

where $\bar{\mathbf{a}}$, $\bar{\mathbf{K}}$, $\bar{\mathbf{F}}$ are respectively the generalized nodal displacements, element tangent stiffness matrix and generalized nodal forces, in the global coordinates system.

The Newton-Raphson method, modified Newton-Rapson method or the artificial time integration method (Liu 2007a, 2007b; Liu and Atluri 2008) can be employed to solve Eqs.(59) and (74). In this implementation, the Newton-Raphson algorithm is used. In all examples, the assumptions of linear trial functions of the rotations were employed, except where stated otherwise.

5 Numerical examples

5.1 Buckling of a beam

The (12×12) tangent stiffness matrix for a beam in space should be capable of predicting buckling under compressive axial loads, when such an axial load interacts with the transverse displacement in the beam. We consider a simply supported beam subject to an axial force as shown in Fig.3 and assume that $EI = 1$ and $L = 1$.

The buckling loads of the beam obtained by the present method using different numbers of elements are shown in Tab.1. It is seen that the buckling load predicted by the present method agrees well with the analytical solution (buckling load is π^2).

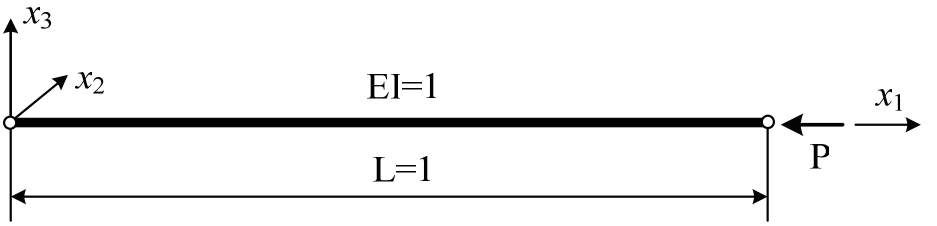

Figure 3: A simply supported beam subject to an axial force

Table 1: Buckling load of the simply supported beam

	Present method(Number of elements)					Analytical solution
	1	2	3	4	10	
Buckling load	12.005	12.005	10.799	10.384	9.950	9.870

When the beam is fixed at $x_1 = 0$, while at the other end it is free and under a compressive load P, the buckling load of the beam obtained by the present method using different number of elements is shown in Tab.2 (the analytical solution is $\frac{\pi^2 EI}{4L^2}$).

Table 2: Buckling load of the beam fixed at $x_1 = 0$

	Present method(Number of elements)					Analytical solution
	1	2	3	4	10	
Buckling load	3.0003	2.5967	2.5240	2.4994	2.4722	2.4674

5.2 Large deformation analysis of a cantilever beam with a symmetric cross section

A large deflection and moderate rotation analysis of a cantilever beam subject to a transverse load at the tip, as shown in Fig. 5, is considered. The cross section of the beam is a square with $h = 1$. The Poisson's ration is $\nu = 0.3$. Fig.5 shows the results obtained in the analysis of the cantilever problem. It is seen that the present results using 10 elements agree well with those of Bathe and Bolourchi (1979).

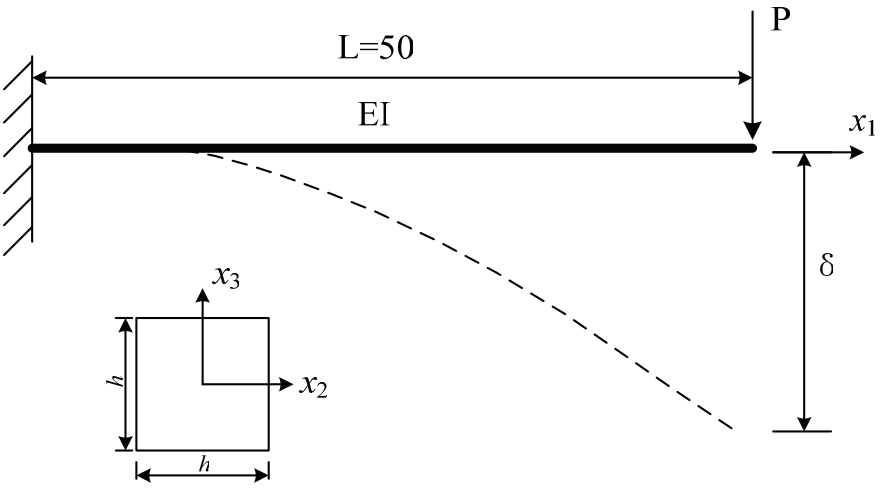

Figure 4: A cantilever beam subject to a transverse load at the tip

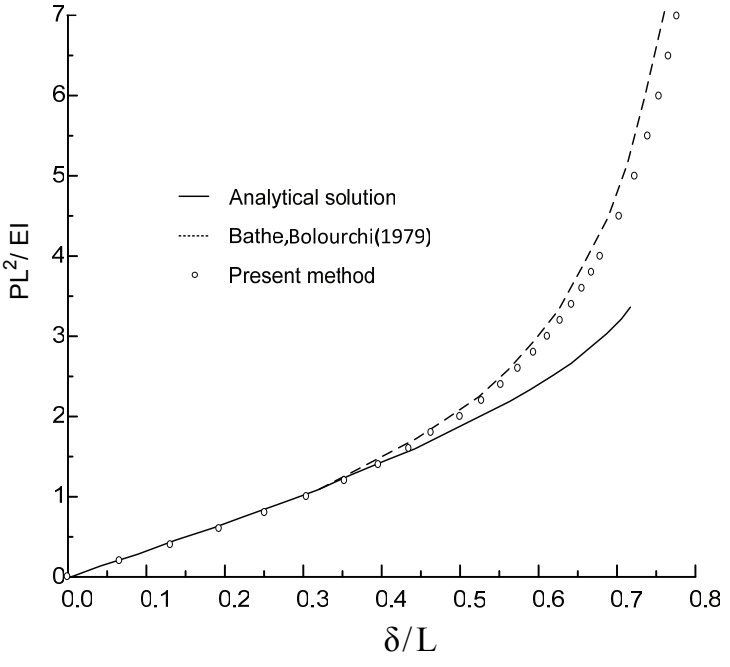

Figure 5: Deflections of a cantilever under a concentrated load

5.3 Large rotations of a cantilever subject to an end-moment and a transverse load

An initially-straight cantilever subject to an end moment $M^* = \frac{ML}{2\pi EI}$ (Crisfield 1990) as shown in Fig.6, is considered. The beam is divided into 10 equal elements. When $M^* = 1$, the beam is curled into a complete circle as shown in Fig.6.

If a non-conservative, follower-type transverse load $P^* = \frac{PL^2}{2\pi EI}$ is applied at the tip, instead of M^*, the initial and deformed geometries of the cantilever are shown in Fig.7.

5.4 Large deformation analysis of a cantilever beam with an asymmetric cross section

We consider the large deflection of a cantilever beam with an asymmetric cross section, as shown in Fig.8. The Poisson's ration is $\nu = 0.3$. The areas of the symmetric and asymmetric cross section in Fig.8 are all equal to 1.

Fig.9 shows the comparison of the deflections in x_3 direction, between the cases of symmetric and asymmetric cross sections. Fig.10 shows the deflection in x_2 direction for the cantilever beam with an asymmetric cross section. However, the deflections in x_2 direction are zero in the case of a symmetric cross section.

5.5 Large displacement analysis of a 45-degree space bend

The large displacement response of a 45-degree bend subject to a concentrated end load [Bathe and Bolourchi (1979)] is calculated as shown in Fig.11. The radius of the bend is 100, the cross section area is 1 and lies in the $x_1 - x_2$ plane. The concentrated is applied in the x_3 direction.

8 equal straight elements and 140 equal load steps are used in the analysis of the problem. Fig.12 shows the tip deflection predicted by the present method and Bathe and Bolourchi (1979). It can be seen that the results of the present method agree excellently with the results of Bathe and Bolourchi (1979).

5.6 A framed dome

A framed dome shown in Fig.13 is considered (Shi and Atluri 1988). A concentrated vertical load P is applied at the crown point. Each member of the dome is modeled by 4 elements.

The linear approaches of the displacements in Eq.(42) are robust for most cases in the large deformation analysis of the space frames. However, the solution was found to diverge when $\lambda > 0.59$ by using the linear interpolations for rotations

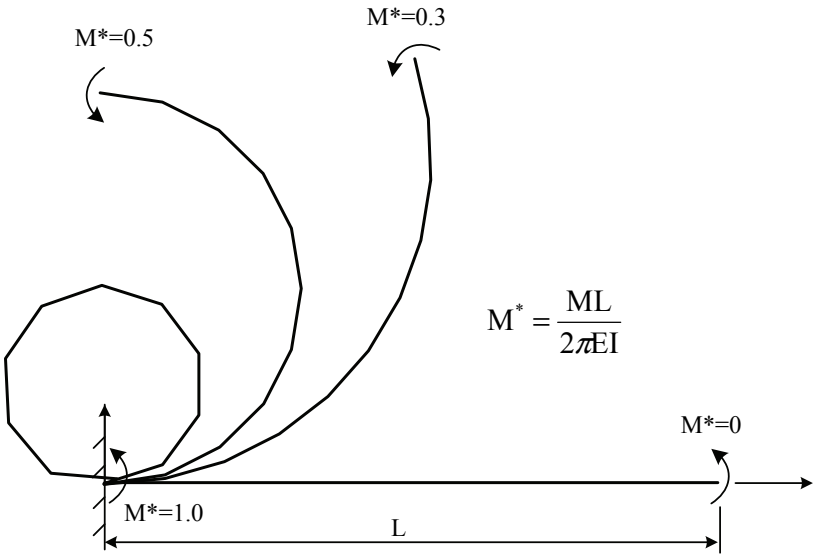

Figure 6: Initial and deformed geometries for cantilever subject to an end-moment

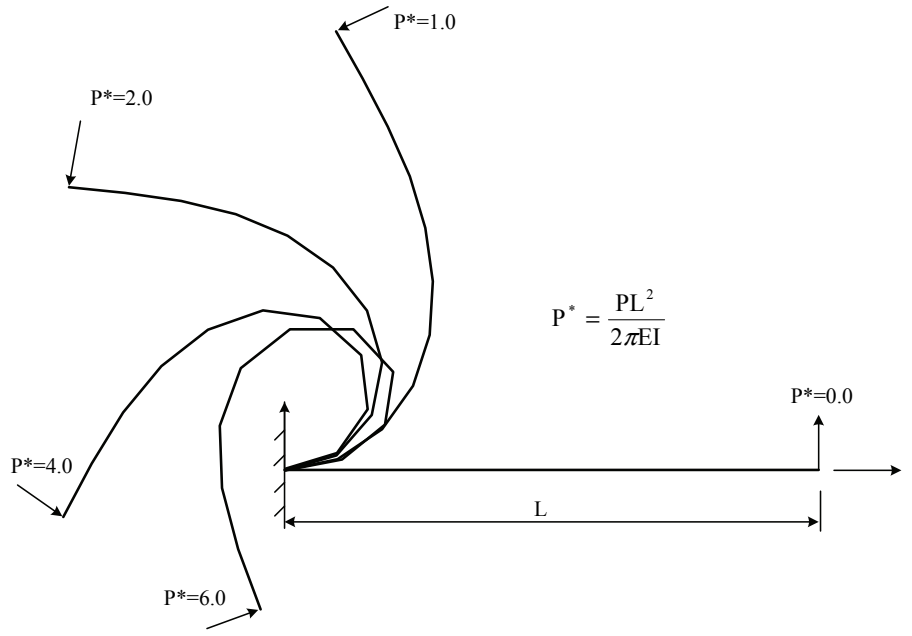

Figure 7: Initial and deformed geometries for cantilever subject to a transverse load

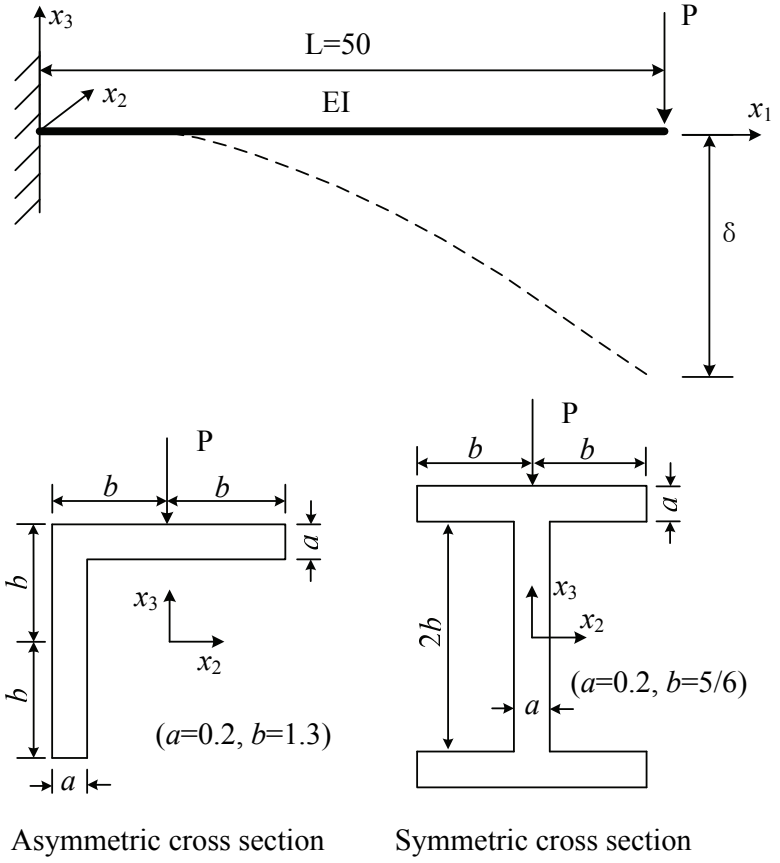

Figure 8: A cantilever beam with an asymmetric cross section

for this example. Thus, the nonlinear stiffness matrix in Eq.(75), which is derived from cubic trial functions of the displacements, was used, and the converged results shown in Fig.14 were obtained.

6 Conclusions

Based on the Reissner variational principle and a von Karman type nonlinear theory in a rotated reference frame, a simplified finite deformation theory of a cylindrical rod subjected to bending and torsion has been developed. The present (12×12) symmetric explicit tangent stiffness matrices of the beam are much simpler than those of many others based on the primal approach or potential energy approach.

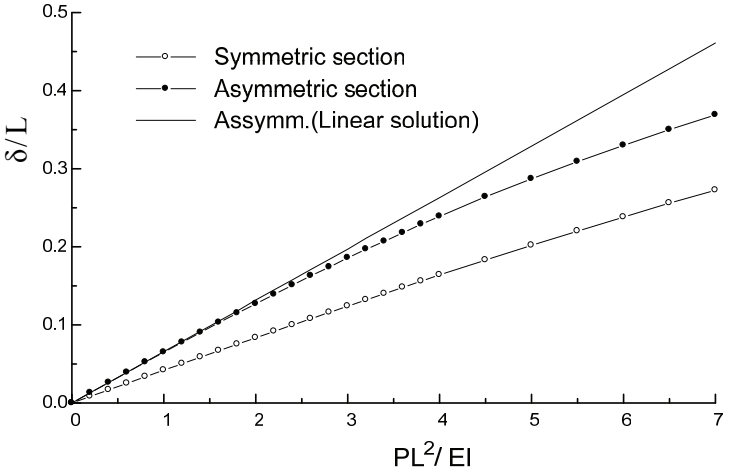

Figure 9: Comparison of the deflections in x_3 direction of a cantilever beam

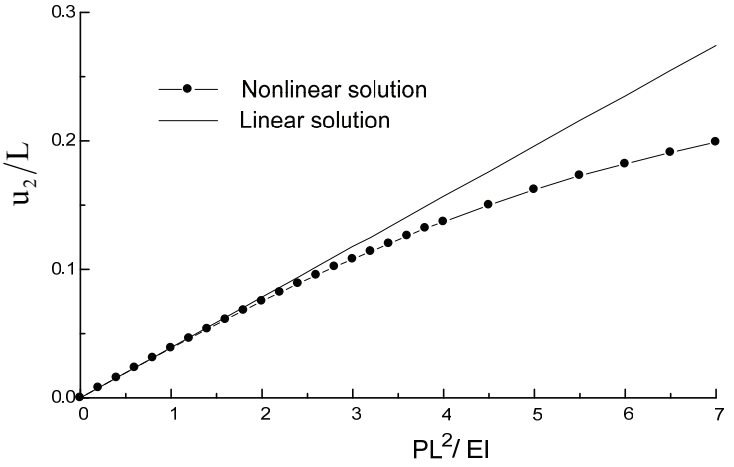

Figure 10: Deflections in x_2 direction for the cantilever beam with asymmetric cross section

The explicit expressions for the tangent stiffness matrix of each element can be seen to be derived as text-book examples of nonlinear analyses. The proposed method is capable of handling large rotation geometrically nonlinear analysis of frames with arbitrary cross sections, which haven't been considered by a majority of previous studies. Numerical examples demonstrate that the present method is just as competitive as the existing methods in terms of accuracy and efficiency.

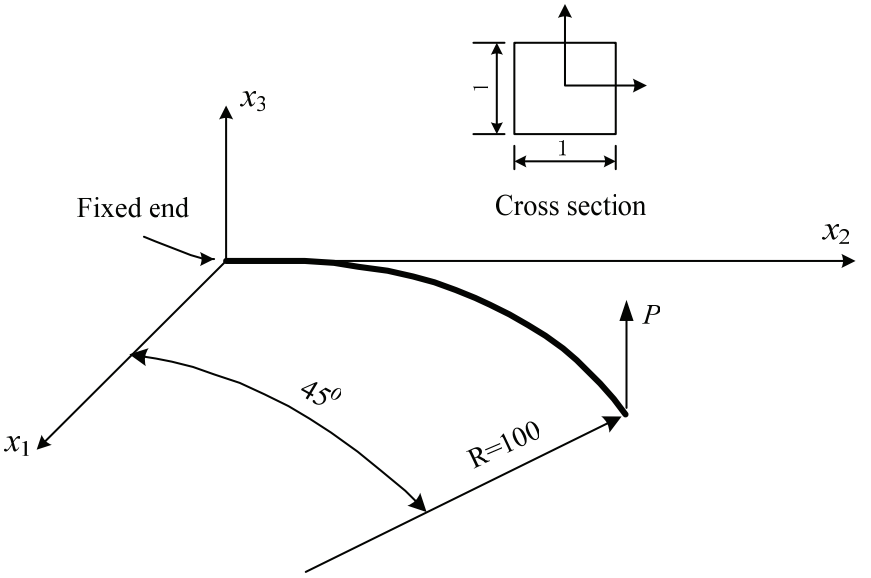

Figure 11: Model of a 45-degree circular bend

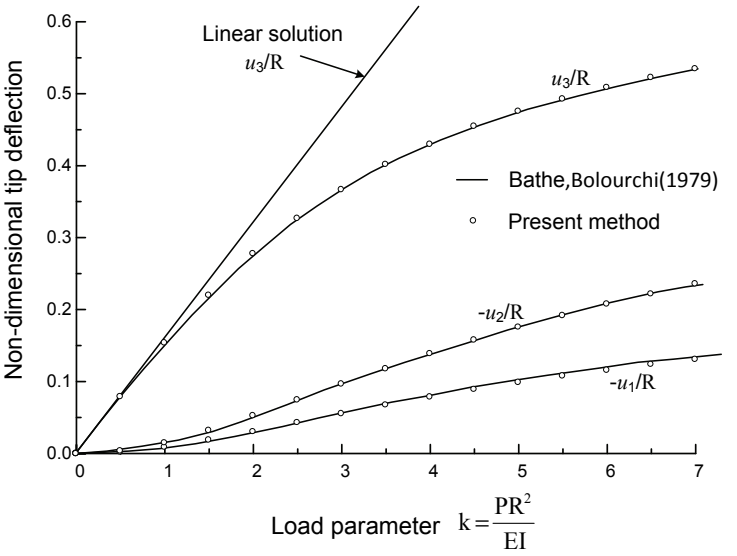

Figure 12: Three-dimensional large deformation of a 45-degree circular bend

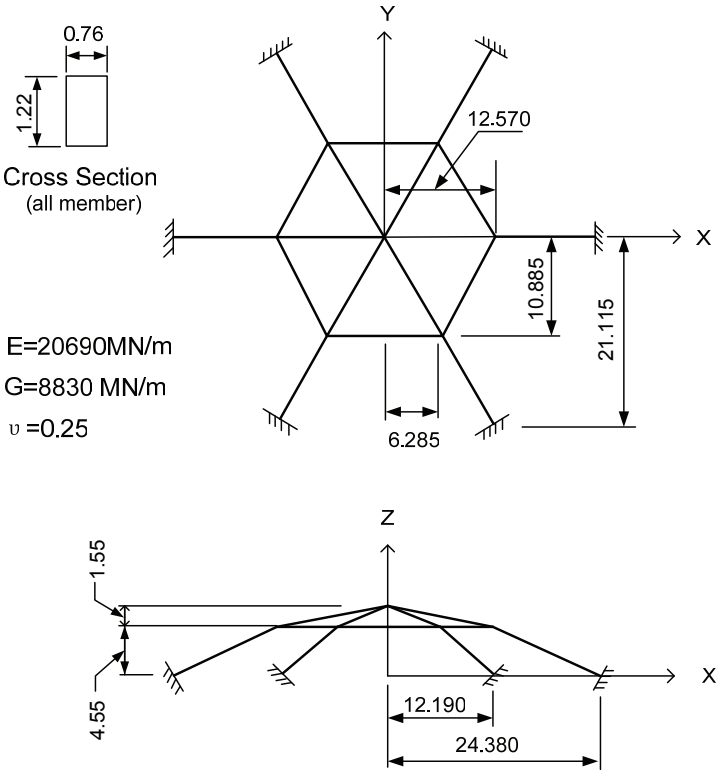

Figure 13: Framed dome (the unit of length is metre)

The present method can be extended to consider the formation of plastic hinges in each beam of the frame; and also to consider large-rotations of plates and shells, by implementing only a von Karman type nonlinear theory in the co-rotational reference frame of each beam/plate element. It is noted that the present approach does not involve any reduced integration, or suppression of Kinematic modes.

Acknowledgement: The authors gratefully acknowledge the support of the Nature Science Foundation of China (NSFC, 10972161). This research was also supported by the World Class University (WCU) program through the National Research Foundation of Korea funded by the Ministry of Education, Science and Technology (Grant no.: R33-10049). The second author is also pleased to acknowledge the support of the Lloyd's Register Educational Trust (LRET) which is an independent charity working to achieve advances in transportation, science, engi-

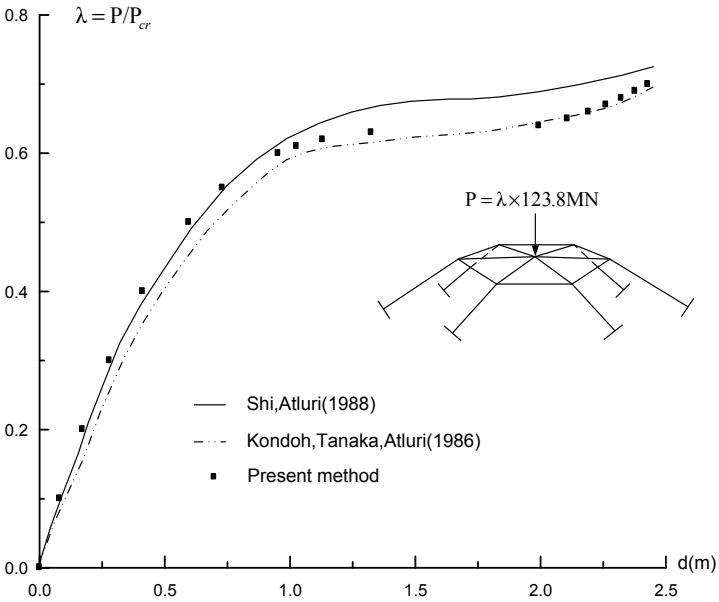

Figure 14: Force-displacement curve for the crown point of a framed dome

neering and technology education, training and research worldwide for the benefit of all.

References

Atluri, S.N. (1975): On 'hybrid' finite element models in solid mechanics, Advances in computer methods for partial differential equations, R. Vichrevetsky, Ed., AICA, pp. 346-355.

Atluri, S.N. (1979): On rate principles for finite strain analysis of elastic and inelastic nonlinear solids, Recent research on mechanical behavior, University of Tokyo Press, pp. 79-107.

Atluri, S.N. (1980): On some new general and complementary energy theorems for the rate problems in finite strain, classical elastoplasticity. *Journal of Structural Mechanics*, Vol. 8(1), pp. 61-92.

Atluri, S.N. (1984): Alternate stress and conjugate strain measures, and mixed variational formulations involving rigid rotations, for computational analyses of finitely deformed plates and shells: part-I: thoery. *Computers & Structures*, Vol. 18(1), pp. 93-116.

Atluri, S.N.; Cazzani, A. (1994): Rotations in computational solid mechanics, invited feature article. *Archives for Computational Methods in Engg*., ICNME, Barcelona, Spain, Vol 2(1), pp. 49-138.

Atluri, S. N.; Gallagher, R. H.; Zienkiewicz, O. C. (Editors). (1983): Hybrid & Mixed Finite Element Methods, J. Wiley & Sons, 600 pages.

Atluri, S.N.; Iura, M.; Vasudevan, S.(2001): A consistent theory of finite stretches and finite rotations, in space-curved beams of arbitrary cross-section. *Computational Mechanics*, vol.27, pp.271-281

Atluri, S.N.; Murakawa, H. (1977): On hybrid finite element models in nonlinear solid mechanics, finite elements in nonlinear mechanics, P.G. Bergan et al, Eds., Tapir Press, Norway, vol. 1, pp. 3-40.

Atluri, S.N.; Reissner, E. (1989): On the formulation of variational theorems involving volume constraints. *Computational Mechanics*, vol. 5, pp 337-344.

Auricchio, F.; Carotenuto, P.; Reali, A. (2008): On the geometrically exact beam model: A consistent, effective and simple derivation from three-dimensional finite-elasticity. *International Journal of Solids and Structures*, vol.45, pp. 4766–4781.

Bathe, K.J.; Bolourchi, S. (1979): Large displacement analysis of three- dimensional beam structures. *International Journal for Numerical Methods in Engineering,* vol.14, pp.961-986.

Cai, Y.C.; Paik, J.K.; Atluri S.N. (2010): Large deformation analyses of space-frame structures, with members of arbitrary cross-section, using explicit tangent stiffness matrices, based on a von Karman type nonlinear theory in rotated reference frames. *CMES: Computer Modeling in Engineering & Sciences*, vol. 53, no. 2, pp. 123-152.

Chan, S.L. (1996): Large deflection dynamic analysis of space frames. *Computers & Structures*, vol. 58, pp.381-387.

Crisfield, M.A. (1990): A consistent co-rotational formulation for non-linear, three-dimensional, beam-elements. *Computer Methods in Applied Mechanics and Engineering*, vol.81, pp. 131–150.

Dinis, L.W.J.S.; Jorge, R.M.N.; Belinha, J. (2009): Large deformation applications with the radial natural neighbours interpolators. *CMES: Computer Modeling in Engineering & Sciences*, vol.44, pp. 1-34

Gendy, A.S.; Saleeb, A.F. (1992): On the finite element analysis of the spatial response of curved beams with arbitrary thin-walled sections. *Computers & Structures*, vol.44, pp.639-652

Han, Z.D.; Rajendran, A.M.; Atluri, S.N. (2005): Meshless Local Petrov- Galerkin (MLPG) approaches for solving nonlinear problems with large deformations and

rotations. *CMES: Computer Modeling in Engineering & Sciences*, vol.10, pp. 1-12

Iura, M.; Atluri, S.N. (1988): Dynamic analysis of finitely stretched and rotated 3-dimensional space-curved beams. *Computers & Structures*, Vol. 29, pp.875-889

Izzuddin, B.A. (2001): Conceptual issues in geometrically nonlinear analysis of 3D framed structures. *Computer Methods in Applied Mechanics and Engineering*, vol.191, pp. 1029–1053.

Kondoh, K.; Tanaka, K.; Atluri, S.N. (1986): An explict expression for the tangent-stiffness of a finitely deformed 3-D beam and its use in the analysis of space frames. *Computers & Structures*, vol.24, pp.253-271.

Kondoh, K.; Atluri, S.N. (1987): Large-deformation, elasto-plastic analysis of frames under nonconservative loading, using explicitly derived tangent stiffnesses based on assumed stresses. *Computational Mechanics*, vol.2, pp.1-25.

Lee, M.H.; Chen, W.H. (2009): A three-dimensional meshless scheme with background grid for electrostatic-structural analysis. *CMC: Computers Materials & Continua*, vol.11, pp. 59-77

Lee, S.Y.; Lin, S.M.; Lee, C.S.; Lu, S.Y.; Liu, Y.T. (2008): Exact large deflection of beams with nonlinear boundary conditions.*CMES: Computer Modeling in Engineering & Sciences*, vol.30, pp. 27-36

Lee, S.Y.; Lu, S.Y.; Liu, Y.R.; Huang, H.C. (2008): Exact large deflection solutions for Timoshenko beams with nonlinear boundary conditions. *CMES: Computer Modeling in Engineering & Sciences*, vol.33, pp. 293-312

Lee, S.Y.; Wu, J.S. (2009): Exact Solutions for the Free Vibration of Extensional Curved Non-uniform Timoshenko Beams. *CMES: Computer Modeling in Engineering & Sciences*,vol.40, pp.133-154.

Liu, C. S. (2007a): A modified Trefftz method for two-dimensional Laplace equation considering the domain's characteristic length. *CMES: Computer Modeling in Engineering & Sciences*, vol. 21, pp. 53-66.

Liu, C.S. (2007b): A highly accurate solver for the mixed-boundary potential problem and singular problem in arbitrary plane domain. *CMES: Computer Modeling in Engineering & Sciences*, vol. 20, pp. 111-122.

Liu, C.S.; Atluri, S.N. (2008): A novel time integration method for solving a large system of non-linear algebraic equations. *CMES: Computer Modeling in Engineering & Sciences*, vol.31, pp. 71-83.

Lo, S.H. (1992): Geometrically nonlinear formulation of 3D finite strain beam element with large rotations. *Computers & Structures*, vol.44, pp.147-157

Mata, P.; Oller, S.; Barbat A.H. (2007): Static analysis of beam structures under nonlinear geometric and constitutive behavior. *Computer Methods in Applied*

Mechanics and Engineering, vol.196, pp. 4458–4478.

Mata, P.; Oller, S.; Barbat A.H. (2008): Dynamic analysis of beam structures considering geometric and constitutive nonlinearity. *Computer Methods in Applied Mechanics and Engineering*, vol.197, pp. 857–878.

Punch, E.F.; Atluri, S.N. (1984): Development and testing of stable, invariant, isoparametric curvilinear 2-D and 3-D hybrid-stress elements. *Computer Methods in Applied Mechanics and Engineering*, Vol.47, pp.331-356

Rabczuk, T.; Areias, P. (2006): A meshfree thin shell for arbitrary evolving cracks based on an extrinsic basis. *CMES: Computer Modeling in Engineering & Sciences*,vol.16, pp.115-130.

Reissner, E. (1953): On a variational theorem for finite elastic deformations, *Journal of Mathematics & Physics*, vol. 32, pp. 129-135.

Shaw, A.; Roy, D. (2007): A novel form of reproducing kernel interpolation method with applications to nonlinear mechanics. *CMES: Computer Modeling in Engineering & Sciences*,vol.19, pp.69-98.

Simo, J.C. (1985): A finite strain beam formulation. The three-dimensional dynamic problem. Part I. *Computer Methods in Applied Mechanics and Engineering*, vol. 49, pp.55–70.

Shi, G.; Atluri, S.N. (1988): Elasto-plastic large deformation analysis of space-frames: a plastic-hinge and strss-based explict derivation of tangent stiffnesses. *International Journal for Numerical Methods in Engineering*, vol.26, pp.589-615.

Wen, P.H.; Hon, Y.C. (2007): Geometrically nonlinear analysis of Reissner- Mindlin plate by meshless computation. *CMES: Computer Modeling in Engineering & Sciences*, vol.21, pp.177-191.

Wu, T.Y.; Tsai, W.G.;Lee, J.J. (2009):Dynamic elastic-plastic and large deflection analyses of frame structures using motion analysis of structures. *Thin-Walled Structures*, vol.47, pp. 1177-1190.

Xue, Q.; Meek J.L. (2001): Dynamic response and instablity of frame structures. *Computer Methods in Applied Mechanics and Engineering*, vol.190, pp. 5233–5242.

Zhou, Z.H.; Chan,S.L. (2004a): Elastoplastic and Large Deflection Analysis of Steel Frames by One Element per Member. I: One Hinge along Member. *Journal of Structural Engineering*, vol. 130, pp.538–544.

Zhou, Z.H.; Chan,S.L. (2004b): Elastoplastic and Large Deflection Analysis of Steel Frames by One Element per Member. II: Three Hinges along Member. *Journal of Structural Engineering*, vol. 130, pp.545–5553.